

Supporting Information

2D-MoS₂/BMN Ceramic Hybrid Structure Flexible TFTs with Tunable Device Properties

Junqing Wei^{1,2}, Shihui Yu¹, Xin Shan³, Kuibo Lan^{1,2}, Xiaodong Yang^{1,2}, Kailiang Zhang^{3,*}, Guoxuan Qin^{1,2,*}

¹School of Microelectronics, Tianjin University, Tianjin 300072, P. R. China

²Tianjin Key Laboratory of Imaging and Sensing Microelectronic Technology, Tianjin University, Tianjin 300072, P. R. China

³School of Electrical and Electronic Engineering, Tianjin Key Laboratory of Film Electronic & Communication Devices, Tianjin University of Technology, Tianjin, 300384, P. R. China

*Corresponding author e-mails: gqin@tju.edu.cn (G. Q.), Kailiang_zhang@163.com (K. Z.)

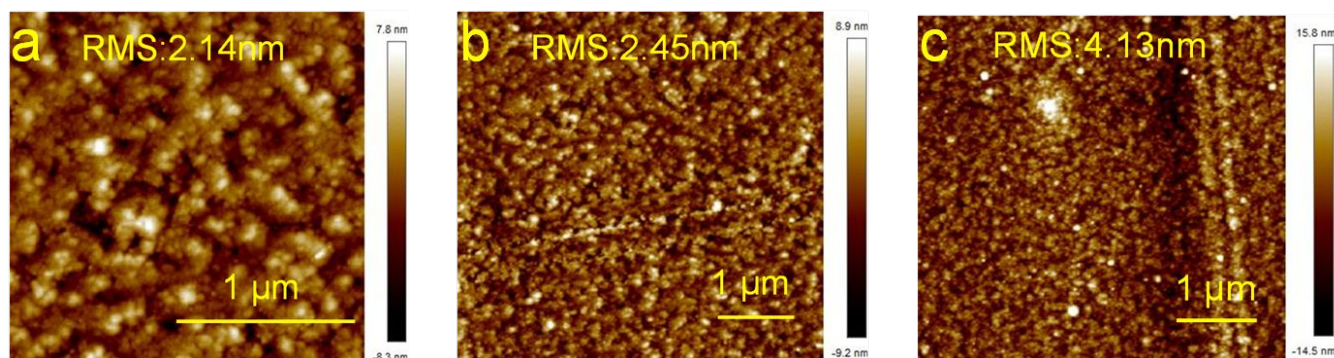


Figure S1. The AFM images of sputtered BMN thin films with topography mode. The topography of sputtered BMN layer in the center region with scanning size of (a) $2\ \mu\text{m} \times 2\ \mu\text{m}$ and (b) $5\ \mu\text{m} \times 5\ \mu\text{m}$, respectively. (c) The topographies of sputtered BMN layer close to the edge region with scanning size of $5\ \mu\text{m} \times 5\ \mu\text{m}$.

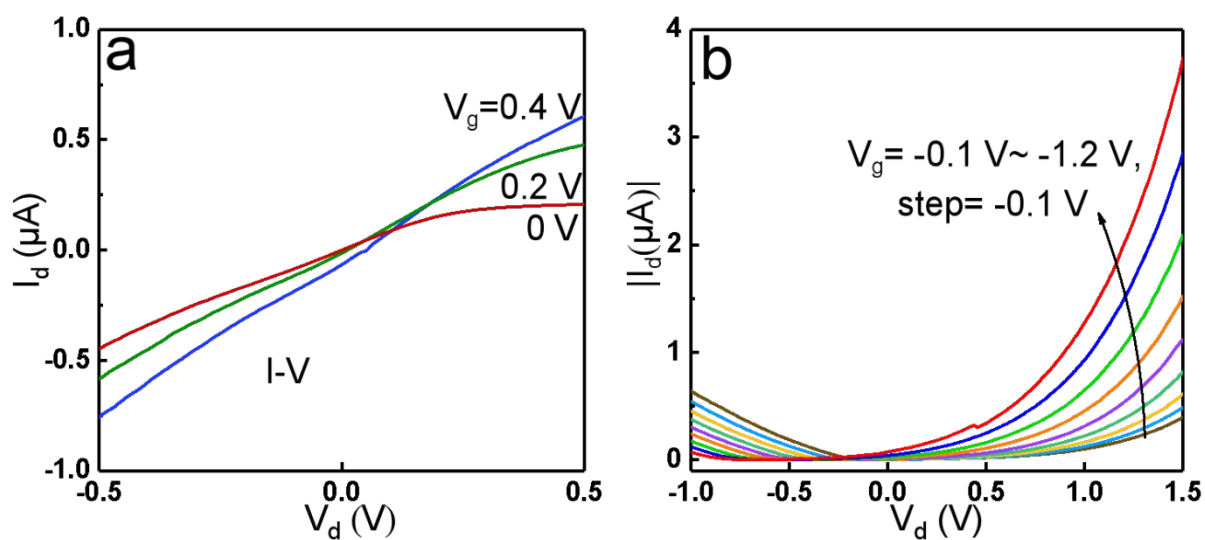


Figure S2. The output characteristics (I_d - V_d) of device type 2 with (a) positive V_g and (b) negative V_g .

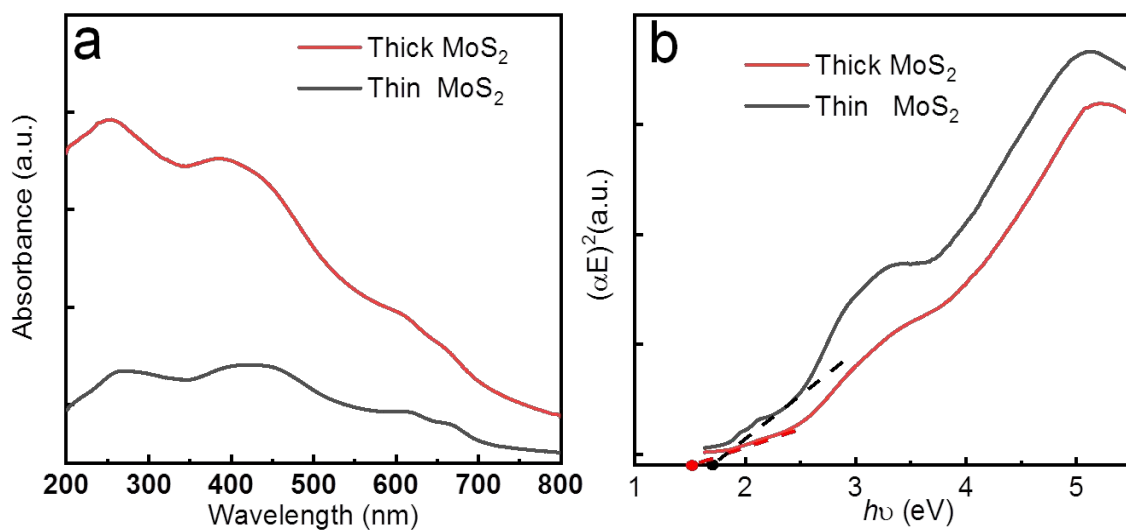


Figure S3. (a) The UV-vis of thin and thick MoS_2 films; (b) The corresponding plots of $(\alpha h\nu)^2$ - $h\nu$ to verify the bandgap of thin and thick MoS_2 films.

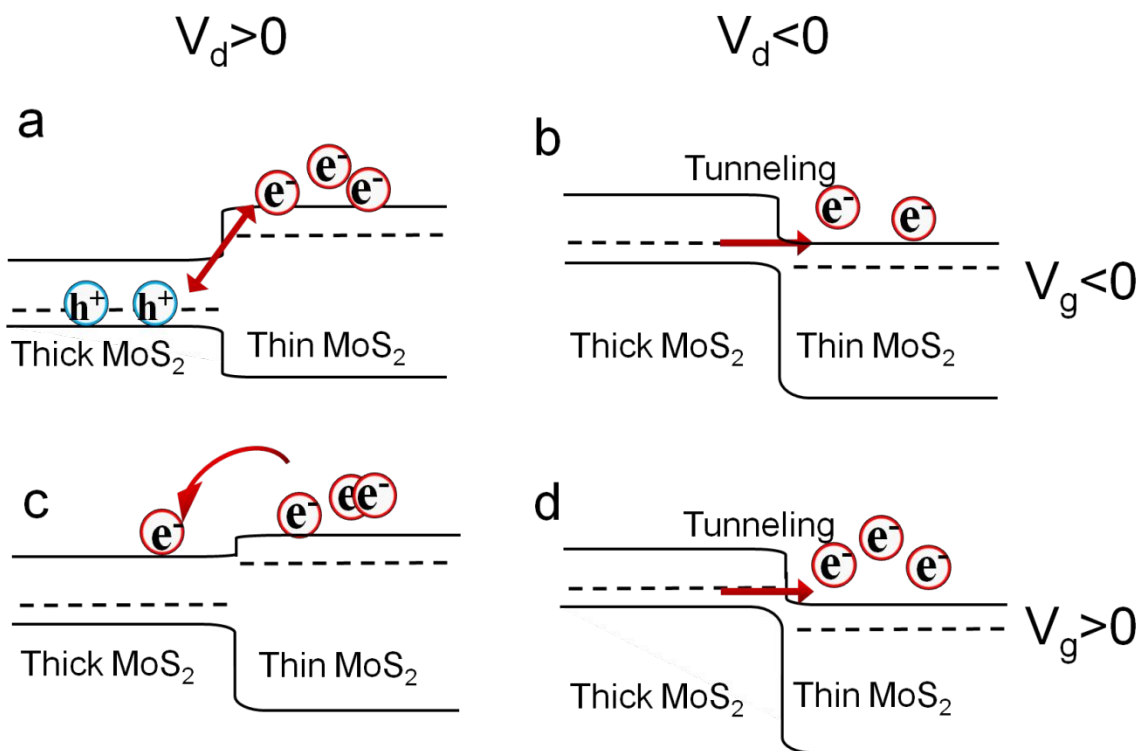


Figure S4. The energy band alignments of the homojunction-MoS₂ device with (a) $V_d > 0$ V and $V_g > 0$ V, (b) $V_d < 0$ V and $V_g > 0$ V, (c) $V_d > 0$ V and $V_g < 0$ V, (d) $V_d < 0$ V and $V_g < 0$ V, respectively. (drawn not to scale)

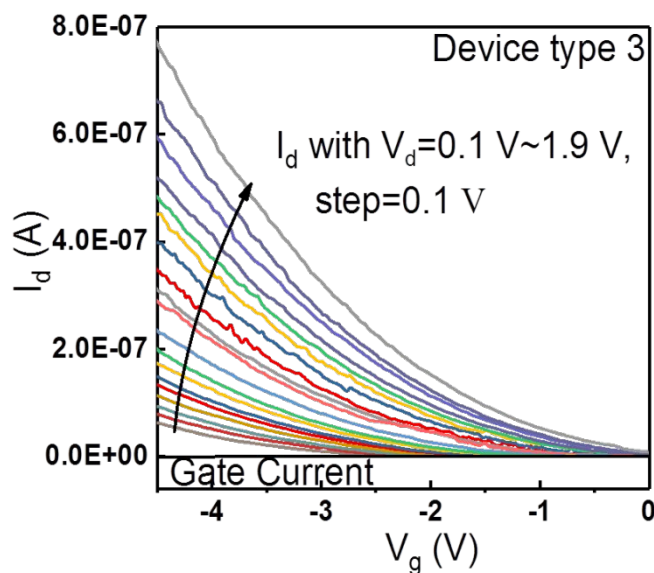


Figure S5. The transfer properties of device type 3 based on thick MoS₂ (~62 nm).

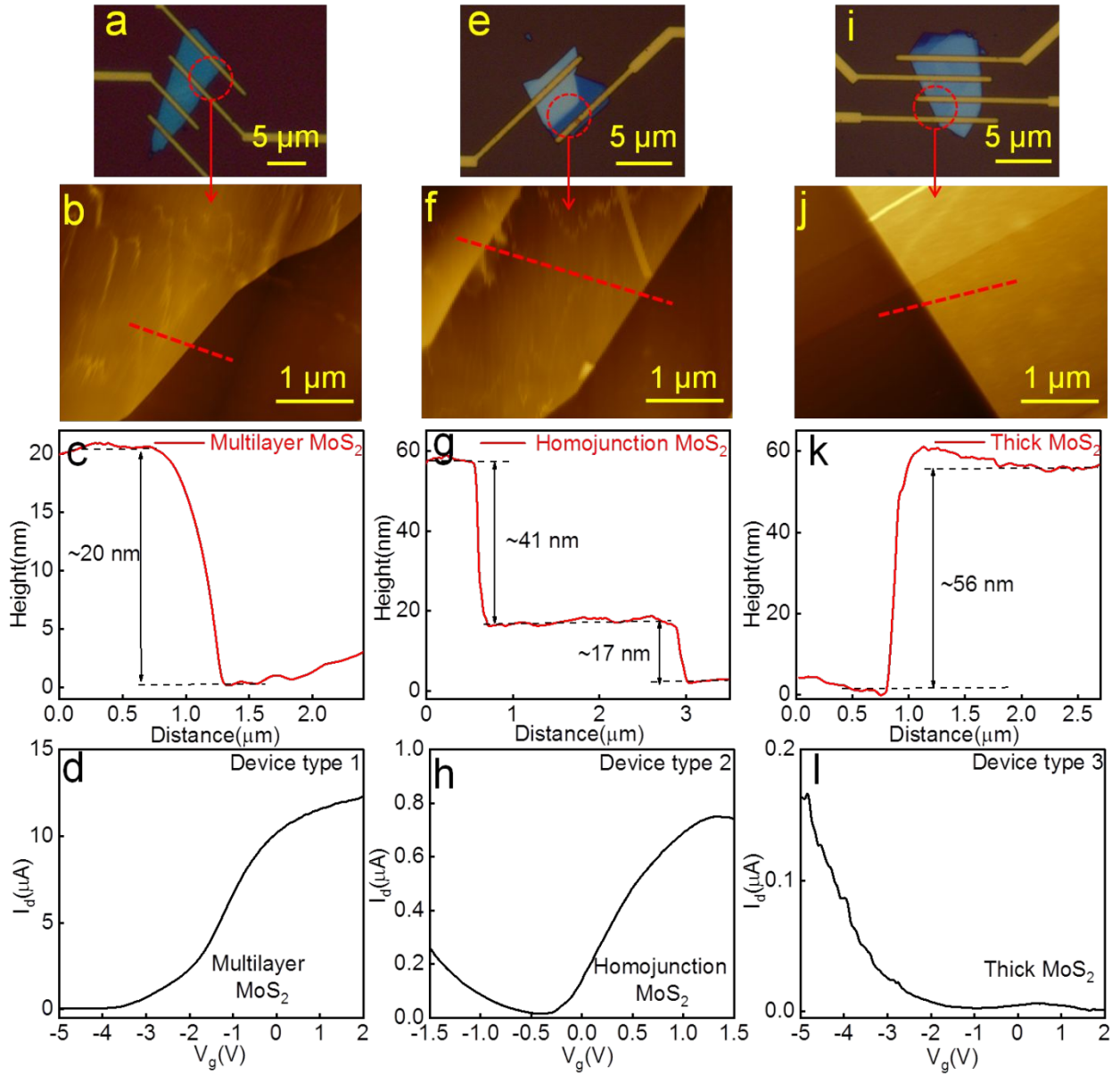


Figure S6. (a) The microscopic image of the multilayer MoS₂ TFT. (b) AFM image of the channel region in the multilayer MoS₂ TFT. (c) The thickness of ~20 nm MoS₂ in the multilayer MoS₂ TFT measured by AFM. (d) The transfer characteristics of the multilayer MoS₂ TFT (device type 1). (e) The microscopic image of the homojunction MoS₂ TFT. (f) AFM image of the channel region in the homojunction MoS₂ TFT. (g) The MoS₂ films in the homojunction MoS₂ TFT with thickness of ~17 nm and ~58 nm, respectively, measured by AFM. (h) The transfer characteristics of the homojunction MoS₂ TFT (device type 2). (i) The microscopic image of the thick MoS₂ TFT. (j) AFM image of the channel region in the thick MoS₂ TFT. (k) The thickness of ~56 nm MoS₂ in the thick MoS₂ TFT measured by AFM. (l) The transfer characteristics of the thick MoS₂ TFT (device type 3).